

# Reactivity of the Verdoheme Analogues. Opening of the Planar Macrocycle by Amide and Thiolate Nucleophiles To Form Helical Complexes

James A. Johnson, Marilyn M. Olmstead, and Alan L. Balch\*

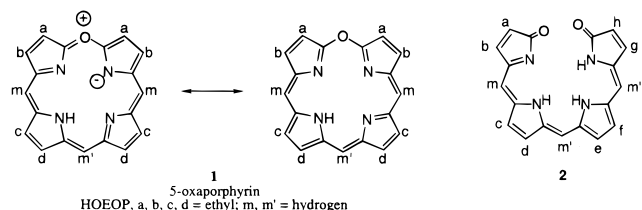
Department of Chemistry, University of California, Davis, California 95616

Received April 20, 1999

The 5-oxaporphyrin macrocycle is a modified porphyrin that has an oxygen atom in place of one *meso*-methine group. These 5-oxaporphyrins are readily produced from heme degradation by both chemical and biological processes. Treatment of metal complexes of 5-oxaporphyrins with nucleophiles can lead to reactions either at the metal or on the ligand. Here we report that the diamagnetic zinc(II) verdoheme analogue  $[\text{Zn}^{\text{II}}(\text{OEOP})](\text{O}_2\text{CCH}_3)$  {OEOP is the monoanion of octaethyl-5-oxaporphyrin} reacts with dimethylamide and with methanethiolate to form ring-opened products  $\text{Zn}^{\text{II}}(\text{OEBNMe}_2)$  and  $\text{Zn}^{\text{II}}(\text{OEBsMe})$ . The ring-opened products have been subjected to crystallographic study. In both complexes the helical tetrapyrrole ligand imposes a structure in which the zinc ion is trapped between planar and tetrahedral coordination. The structures of these two complexes are compared with that of  $\text{Zn}^{\text{II}}(\text{OEBOMe})$ , which has a similar helical shape.

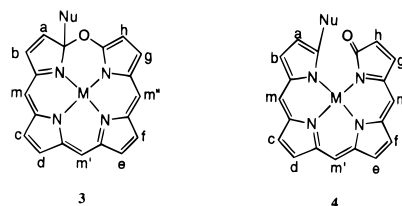
## Introduction

Verdohemes,<sup>1–4</sup> the green iron(II) complexes of the 5-oxaporphyrin macrocycle **1**<sup>5</sup> are produced by oxidative destruction of hemes by either heme oxygenase<sup>6–8</sup> or the coupled oxidation process in which iron(II) porphyrins in a suitable ligating environment are treated with dioxygen in the presence of a sacrificial reducing agent.<sup>9,10</sup> A related process has been developed for cobalt(II) porphyrins.<sup>11,12</sup> With zinc and iron, verdoheme-type complexes can also be formed by cyclization of biliverdin, **2**.<sup>13,14</sup> Thus, iron, cobalt, and zinc complexes of 5-oxaporphyrins have been prepared.<sup>13–16</sup>



The reactivity of metal complexes with 5-oxaporphyrin ligands still involves a number of ill-defined reactions. It has been established that both metal-centered and ligand-centered

reactions can occur. Metal-centered reactions that produce changes in metal oxidation state as well as changes in axial ligation have been shown to occur for iron<sup>4,5</sup> and cobalt<sup>7,8</sup> 5-oxaporphyrin complexes without alteration of the 5-oxaporphyrin macrocycle. Although the 5-oxaporphyrin macrocycle markedly resembles the corresponding porphyrin, it is much more vulnerable to attack by anionic nucleophiles. The products of nucleophilic addition have been formulated as either closed macrocycles, **3**, with the nucleophile attached to a carbon atom adjacent to the 5-oxa group, or as open-chain tetrapyrroles, **4**.

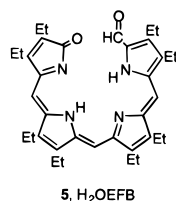


These two structures cannot be readily differentiated through analysis of their NMR spectra alone. Both structures contain four distinct pyrrolic rings and three different *meso*-carbon atoms. Consequently both structures are expected to produce similar patterns of resonances. Previous work from this laboratory has conclusively shown that treatment of iron(II), cobalt(II), and zinc(II) complexes of the 5-oxaporphyrins with alkoxide ions results in ring opening to produce metal complexes that contain the dianion of the open chain tetrapyrrole **4** with Nu = OR.<sup>17,18</sup> Mechanistically, it is likely that the formation of **3**, with its tetrahedral carbon atom, precedes formation of **4**.

- (1) Lagarias, J. C. *Biochim. Biophys. Acta* **1982**, 717, 12.
- (2) Balch, A. L.; Latos-Grażyński, L.; Noll, B. C.; Olmstead, M. M.; Szterenber, L.; Safari, N. *J. Am. Chem. Soc.* **1993**, 115, 1422.
- (3) Balch, A. L.; Noll, B. C.; Safari, N. *Inorg. Chem.* **1993**, 32, 2901.
- (4) Balch, A. L.; Koerner, R.; Olmstead, M. M. *J. Chem. Soc., Chem. Commun.* **1995**, 873.
- (5) Abbreviations used: H<sub>2</sub>OEP, octaethylporphyrin; HOEOP, octaethyl-5-oxaporphyrin; H<sub>3</sub>OEB, octaethylbilindione; H<sub>2</sub>OEFB, octaethylformylbiliverdin; H<sub>2</sub>OEBOMe, octaethylmethoxybiliverdin; py, pyridine.
- (6) Maines, M. D. *Heme Oxygenase: Clinical Applications and Functions*; CRC Press: Boca Raton, FL, 1992.
- (7) Bissell, D. M. In *Liver: Normal Function and Disease. Bile Pigments and Jaundice*; Ostrow, J. D., Ed.; Marcel Dekker: New York, 1986; Vol. 4, p 133.
- (8) Ortiz de Montelano, P. R. *Acc. Chem. Res.* **1998**, 31, 543.
- (9) Balch, A. L.; Koerner, R.; Latos-Grażyński, L.; Lewis, J. E.; St. Claire, T. N.; Zovinka, E. P. *Inorg. Chem.* **1997**, 36, 3892.
- (10) St. Claire, T. M.; Balch, A. L. *Inorg. Chem.* **1999**, 38, 684.

- (11) Balch, A. L.; Mazzanti, M.; Olmstead, M. M. *J. Chem. Soc., Chem. Commun.* **1994**, 269.
- (12) Balch, A. L.; Mazzanti, M.; St. Claire, T. M.; Olmstead, M. M. *Inorg. Chem.* **1995**, 34, 2194.
- (13) Saito, S.; Itano, H. A. *J. Chem. Soc., Perkin Trans. 1* **1986**, 1.
- (14) Fuhrhop, J.-H.; Salek, A.; Subramanian, J.; Mengersen, C.; Besecke, S. *Leibigs Ann. Chem.* **1975**, 1131.
- (15) Fuhrhop, J.-H.; Krüger, P.; Sheldrick, W. S. *Leibigs Ann. Chem.* **1977**, 339.
- (16) Fuhrhop, J.-H.; Krüger, P. *Leibigs Ann. Chem.* **1977**, 360.
- (17) Koerner, R.; Latos-Grażyński, L.; Balch, A. L. *J. Am. Chem. Soc.* **1998**, 120, 9246.

Both **3** and **4** represent chiral molecules whose chirality arises from the presence of a tetrasubstituted carbon atom in **3** or a helical arrangement of the open tetrapyrrole in **4**. In **4** the overlap of the Nu addendum and the terminal lactam function prevents the tetrapyrrole from assuming a planar structure. A number of metal complexes of open chain tetrapyrrole ligands that are related to **4** have been studied previously. These complexes include molecules obtained from octaethylbilindione, **2**, with  $a-h = Et (H_3OEB)^{12,19-25}$  and from octaethylformylbiliverdin, **5** ( $H_2OEFB$ ).<sup>26</sup> These ligands can also produce four-coordinate



complexes with a helical twist in the ligand portion. Complexes of Cu(II), Ni(II), and Co(II) with octaethylformylbiliverdin, **5**, as the ligand behave much like their porphyrin counterparts.<sup>27</sup> However, complexes prepared from octaethylbilindione, **2**, have unusual electronic structures that reflect the ability to change the redox states of both the metal and the ligand. Thus, some of the metal complexes of  $H_3OEB$  exhibit significant ligand radical character.

Here we examine the reactivity of the zinc verdoheme [ $Zn^{II}(OEOP)](O_2CCH_3)$  toward two other nucleophiles, dimethylamide and methanethiolate. Earlier work has shown that reaction of verdoheme itself with ammonia can be conducted to produce the 5-azaporphyrin macrocycle,<sup>27,28</sup> and our work with dimethylamide was conducted to provide insight into this reaction as well as to determine whether the adduct, if formed, had structure **3** or **4**. In the case of thiolate addition, one study indicated that the open chain complex of type **4** formed,<sup>16</sup> while another study indicated on the basis of spectroscopic information that addition led to the formation of the closed product **3**.<sup>29</sup> Since no compound containing this structural entity has yet been fully structurally characterized, we were eager to pursue this issue. To facilitate isolation of these adducts, nucleophilic additions to the zinc complex [ $Zn^{II}(OEOP)](O_2CCH_3)$  were studied, since previous work indicated that the zinc complexes were significantly more stable than their cobalt(II) and iron(II) analogues.

- (18) Latos-Grażyński, L.; Johnson, J.; Attar, S.; Olmstead, M. M.; Balch, A. L. *Inorg. Chem.* **1998**, *37*, 4493.  
 (19) Balch, A. L.; Mazzanti, M.; Noll, B. C.; Olmstead, M. M. *J. Am. Chem. Soc.* **1993**, *115*, 12206.  
 (20) Balch, A. L.; Mazzanti, M.; Noll, B. C.; Olmstead, M. M. *J. Am. Chem. Soc.* **1994**, *116*, 9114.  
 (21) Attar, S.; Balch, A. L.; Van Calcar, P. M.; Winkler, K. *J. Am. Chem. Soc.* **1997**, *119*, 3317.  
 (22) Attar, S.; Ozarowski, A.; Van Calcar, P. M.; Winkler, K.; Balch, A. L. *Chem. Commun.* **1997**, 1115.  
 (23) Bonnett, R.; Buckley, D. G.; Hamzetaash, D. *J. Chem. Soc., Perkin Trans. 1* **1981**, 322.  
 (24) Bonfiglio, J. V.; Bonnett, R.; Buckley, D. G.; Hamzetaash, D.; Hursthouse, M. B.; Malik, K. M. A.; McDonagh, A. F.; Trotter, J. *Tetrahedron* **1983**, *39*, 1865.  
 (25) Balch, A. L.; Latos-Grażyński, L.; Noll, B. C.; Olmstead, M. M.; Safari, N. *J. Am. Chem. Soc.* **1993**, *115*, 9056.  
 (26) Koerner, R.; Olmstead, M. M.; Ozarowski, A.; Phillips, S. L.; Van Calcar, P. M.; Winkler, K.; Balch, A. L. *J. Am. Chem. Soc.* **1998**, *120*, 1274.  
 (27) Balch, A. L.; Olmstead, M. M.; Safari, N. *Inorg. Chem.* **1993**, *32*, 291.  
 (28) Saito, S.; Sumita, S.; Iwai, K.; Sano, H. *Bull. Chem. Soc. Jpn.* **1988**, *61*, 3539.  
 (29) Hempenius, M. A.; Koek, J. H.; Lugtenburg, J.; Fokkens, R. *Recl. Trav. Chim. Pays-Bas* **1987**, *106*, 105.

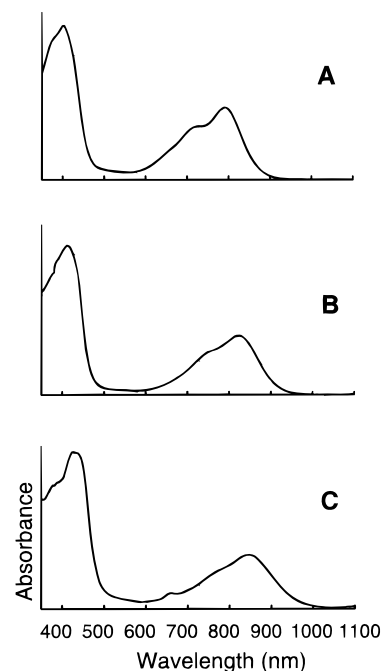
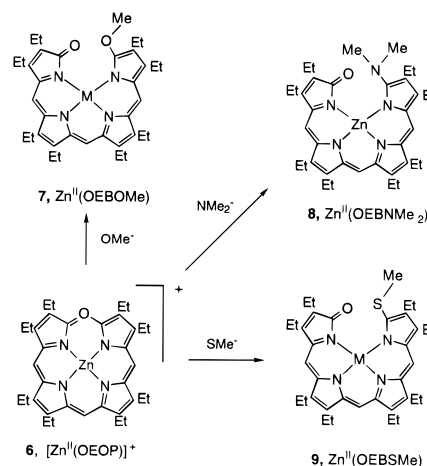


**Figure 1.** Electronic absorption spectra of (A)  $Zn^{II}(OEBOMe)$ , **3**, in dichloromethane solution,  $\lambda_{max}$ , nm ( $\epsilon$ ,  $M^{-1} cm^{-1}$ ) 402 (33 600), 790 (16 000); (B)  $Zn^{II}(OEBNMe_2)$ , **8**, in dichloromethane solution,  $\lambda_{max}$ , nm ( $\epsilon$ ,  $M^{-1} cm^{-1}$ ) 413 (30 800), 822 (12 000); and (C)  $Zn^{II}(OEBSMe)$ , **9**, in dichloromethane solution,  $\lambda_{max}$ , nm ( $\epsilon$ ,  $M^{-1} cm^{-1}$ ) 441 (22 100), 846 (7850).

### Scheme 1



Moreover, complications for redox reactions were minimized by working with the zinc compounds.

### Results

**Synthetic and Spectroscopic Studies.** The zinc(II) verdoheme analogue **6** undergoes ring opening when treated with dimethylamide or methanethiolate as shown in Scheme 1. The reactions are accompanied by a color change from blue-green for the verdoheme complex to yellow or yellow-green for the ring-opened compounds, but both complexes are isolated as dark, nearly black solids. Figure 1 compares the electronic absorption spectrum of the previously characterized ring-opened product  $Zn^{II}(OEBOMe)$  with the corresponding spectra of  $Zn^{II}(OEBNMe_2)$  and  $Zn^{II}(OEBSMe)$ . The spectra show similar features with a broadened peak in the region of the porphyrin Soret band at 400 nm and a broad, low-energy absorption in the 800 nm region. The latter feature shows a shoulder at higher

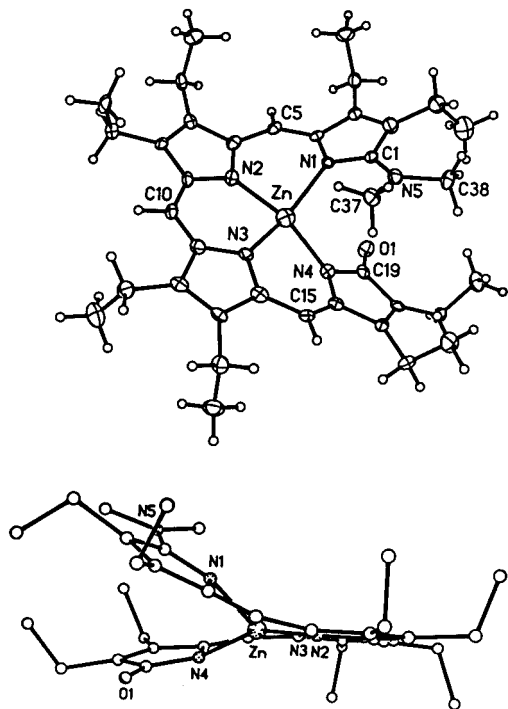


**Figure 2.** Top: A perspective view of  $\text{Zn}^{\text{II}}(\text{OEBNMe}_2)$  with 50% thermal contours for all non-hydrogen atoms and arbitrarily sized circles for the hydrogen atoms. Bottom: A view looking edge-on at the planar portion that consists of the pyrrole rings which contain N(2) and N(3). Hydrogen atoms are omitted, and other atoms are shown as circles.

energies and undergoes a red shift as the ligand addend is altered from OMe to  $\text{NMe}_2$  and to SMe. In contrast the spectrum of the precursor  $[\text{Zn}^{\text{II}}(\text{OEOP})](\text{O}_2\text{CCH}_3)$  shows typical verdoheme-type features with a sharp, low-energy absorption at 652 nm that has an extinction coefficient similar to that of the sharp peak at ca. 400 nm.

The  $^1\text{H}$  NMR spectra (see the Experimental Section) of  $\text{Zn}^{\text{II}}(\text{OEBNMe}_2)$  and  $\text{Zn}^{\text{II}}(\text{OEBSMe})$  are consistent with their structures. In particular, three resonances are observed in either compound for the *meso*-methine protons. Complex multiplets are observed in the regions 2.5–2.0 and 1.2–0.8 ppm for the methylene and methyl protons of the ethyl groups, respectively. In the spectrum of  $\text{Zn}^{\text{II}}(\text{OEBNMe}_2)$ , the  $\text{NMe}_2$  group produces a single resonance at 3.12 ppm at 25 °C. However, upon cooling, this resonance broadens, until at –30 °C two distinct, equally intense resonances at 3.60 and 2.95 ppm are observed. On further cooling, these resonances narrow. These resonance changes are reversed upon warming the sample. The two methyl groups of the  $\text{NMe}_2$  substituent are inequivalent at low temperature because rotation about the N–C(pyrrole) bond is slowed as a result of both steric factors and conjugation (vide infra). For  $\text{Zn}^{\text{II}}(\text{OEBSMe})$  the  $^1\text{H}$  NMR spectrum shows a singlet at 2.86 ppm that is assigned to the protons of the methyl group of the thiolate appendage.

**Crystal and Molecular Structure of  $\text{Zn}^{\text{II}}(\text{OEBNMe}_2)$ .** The structure of  $\text{Zn}^{\text{II}}(\text{OEBNMe}_2)$  has been determined by single-crystal X-ray diffraction. Two perspective views of the complex are shown in Figure 2. Table 1 contains selected interatomic distances and angles.

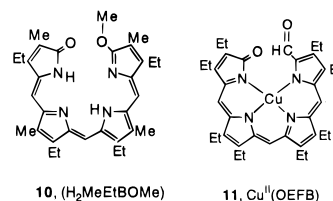
The ligand in  $\text{Zn}^{\text{II}}(\text{OEBNMe}_2)$  has a helical geometry which is similar to the ligand geometry in a number of complexes of open chain tetrapyrrole ligands. Relevant examples of these include  $\text{Zn}^{\text{II}}(\text{OEBOMe})$ ,  $\text{Cu}^{\text{II}}(\text{OEFB})$ ,  $\text{Co}(\text{OEB})$ , and the free ligand  $\text{H}_2\text{MeEtBOMe}$ , **10**.<sup>30</sup> Each of these has a metal ion coordinated by four nitrogen atoms with metal coordination that

**Table 1.** Selected Bond Lengths (Å) and Bond Angles (deg) for  $\text{Zn}^{\text{II}}(\text{OEBOMe})$ ,  $\text{Zn}^{\text{II}}(\text{OEBNMe}_2)$ , and  $\text{Zn}^{\text{II}}(\text{OEBSMe})$

	$\text{Zn}^{\text{II}}(\text{OEBOMe})^a$	$\text{Zn}^{\text{II}}(\text{OEBNMe}_2)$	$\text{Zn}^{\text{II}}(\text{OEBSMe})$
Bond Lengths			
Zn–N(1)	2.102 (3)	2.084 (5)	2.048 (7)
Zn–N(2)	1.979 (2)	2.002 (5)	1.969 (8)
Zn–N(3)	2.015 (3)	2.006 (5)	2.006 (7)
Zn–N(4)	1.976 (2)	2.022 (5)	1.974 (7)
C(19)–O	1.327 (4)	1.220 (8)	1.228 (11)
C(1)–X	1.227 (4)	1.348 (9)	1.732 (10)
Angles (deg)			
N(1)–Zn–N(2)	89.48 (10)	88.3 (2)	90.3 (3)
N(1)–Zn–N(3)	146.25 (10)	146.6 (2)	146.3 (3)
N(1)–Zn–N(4)	101.35 (10)	102.3 (2)	101.9 (3)
N(2)–Zn–N(3)	91.97 (10)	91.7 (2)	91.4 (3)
N(2)–Zn–N(4)	154.01 (10)	155.7 (2)	154.3 (3)
N(3)–Zn–N(4)	91.83 (10)	91.1 (2)	90.7 (3)

<sup>a</sup> Data from Latos-Grażyński, L.; Johnson, J.; Attar, S.; Olmstead, M. M.; Balch, A. L. *Inorg. Chem.* **1998**, *37*, 4493, but renumbered to conform with the numbering system used for  $\text{Zn}^{\text{II}}(\text{OEBNMe}_2)$  and  $\text{Zn}^{\text{II}}(\text{OEBSMe})$ .

is poised between tetrahedral and planar. Although the helical molecules of  $\text{Zn}^{\text{II}}(\text{OEBNMe}_2)$  are chiral, there is a center of symmetry in the space group  $P\bar{1}$ , so each crystal of  $\text{Zn}^{\text{II}}(\text{OEBNMe}_2)$  contains a racemate of the two enantiomeric helices.



The four-coordinate zinc ion has a geometry that is probably best described as a flattened tetrahedron. The Zn–N(1) distance, 2.184(5) Å, is slightly longer than the other Zn–N distances, which fall in the range 2.002(5)–2.022(5) Å. A similar situation exists in  $\text{Zn}^{\text{II}}(\text{OEBOMe})$  and  $\text{Cu}^{\text{II}}(\text{OEFB})$ , **11**, where the M–N bond that involves the ring with the methoxy or formyl substituents is somewhat longer than the other three M–N bonds. The other Zn–N distances are slightly shorter than those found in zinc porphyrins, where the Zn–N distances fall in the range 2.06–2.07 Å.<sup>31</sup>

The angular disposition of nitrogen atoms about the zinc ion is quite irregular. The three N–Zn–N angles that are internal to a chelate ring (88.3(2)°, 91.7(2)°, and 91.1(2)°) are all nearly 90°. The other three are considerably wider, 102.3(2)°, 146.6(2)°, and 155.7(2)°. The same pattern, with one long M–N bond to the pyrrole ring that contains the methoxy or formyl group, is seen in  $\text{Zn}^{\text{II}}(\text{OEBOMe})$  and  $\text{Cu}^{\text{II}}(\text{OEFB})$ .

The environment about N(5) of the dimethylamide group is planar. The C–N(5)–C bond angles C(1)–N(5)–C(37), 122.0(6)°, C(1)–N(5)–C(38), 123.5(6)°, and C(37)–N(5)–C(38), 114.4(5)° are near 120°, and the sum of these three angles is 359.9°. The dimethylamido unit is also nearly coplanar with the adjacent pyrrole ring. The dihedral angle between these two units is only 16.6°. The planarity of N(5) and the orientation of the dimethylamide unit suggest that conjugation within the tetrapyrrole extends out into this functionality and that resonance

(30) Kratky, C.; Jorde, C.; Falk, H.; Thirring, K. *Tetrahedron* **1983**, *39*, 1859.

(31) Scheidt, W. R. In *The Porphyrins*; Dolphin, D., Ed.; Academic Press, New York, 1978; Vol. 3, p 463.

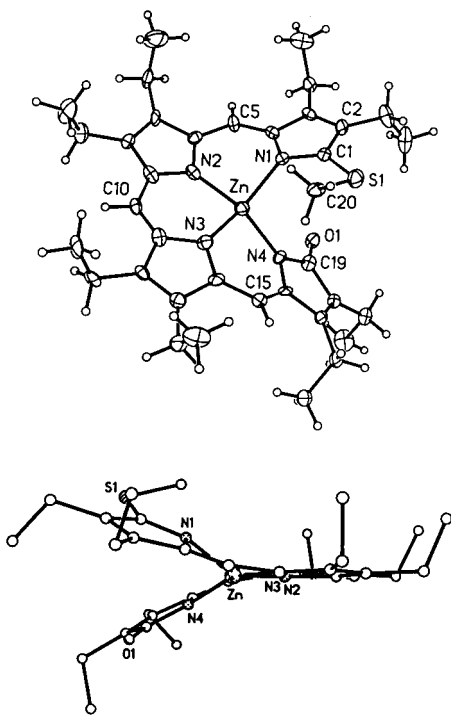
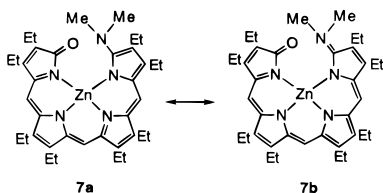


**Figure 3.** A perspective view of  $\text{Zn}^{\text{II}}(\text{OEBSMe})$  with 50% thermal contours for all non-hydrogen atoms and arbitrarily sized circles for the hydrogen atoms. Bottom: A view looking edge-on at the planar portion that consists of the pyrrole rings which contain N(2) and N(3). Hydrogen atoms are omitted, and other atoms are shown as circles.

structure **7b** is particularly important in describing the ligand electronic structure.



**Crystal and Molecular Structure of  $\text{Zn}^{\text{II}}(\text{OEBSMe})$ .** The structure of  $\text{Zn}^{\text{II}}(\text{OEBSMe})$  has also been obtained by X-ray diffraction. Figure 3 shows two perspective views of the complex. Selected interatomic distances and angles are given in Table 1 where they may be compared with those of  $\text{Zn}^{\text{II}}(\text{OEBOMe})$  and  $\text{Zn}^{\text{II}}(\text{OEBNMe}_2)$ .

The ligand in  $\text{Zn}^{\text{II}}(\text{OEBSMe})$  imposes a helical geometry on the complex and a flattened tetrahedral geometry on the zinc ion. Although the helical molecules of  $\text{Zn}^{\text{II}}(\text{OEBSMe})$  are chiral, the space group  $P2_1/n$  is centrosymmetric. Thus, as with  $\text{Zn}^{\text{II}}(\text{OEBNMe}_2)$ , each crystal of  $\text{Zn}^{\text{II}}(\text{OEBSMe})$  contains a racemate of the two enantiomeric helices.

The four-coordinate zinc ion is again situated in a site where one of the four  $\text{Zn}-\text{N}$  distances is slightly longer than the other three. Thus, the  $\text{Zn}-\text{N}(1)$  distance, 2.048(7) Å, which involves the pyrrole ring that bears the methanethiolate addendum, is slightly longer than the other  $\text{Zn}-\text{N}$  distances, which fall in the range 1.974(7)–2.006(7) Å. As with  $\text{Zn}^{\text{II}}(\text{OEBOMe})$  and  $\text{Zn}^{\text{II}}(\text{OEBNMe}_2)$ , the other  $\text{Zn}-\text{N}$  distances are slightly shorter than those found in zinc porphyrins, where the  $\text{Zn}-\text{N}$  distances fall in the range 2.06–2.07 Å.<sup>32</sup>

The angular disposition of nitrogen atoms about the zinc ion is similar to that of  $\text{Zn}^{\text{II}}(\text{OEBNMe}_2)$ . The three  $\text{N}-\text{Zn}-\text{N}$  angles that are internal to a chelate ring (90.3(3)°, 90.7(3)°, and 91.4(3)°) are all nearly 90°. The other three are considerably wider, 101.9(3)°, 146.3(3)°, and 154.3(3)°.

## Discussion

The present study shows that the 5-oxaporphyrin macrocycle in  $[\text{Zn}^{\text{II}}(\text{OEOP})](\text{O}_2\text{CCH}_3)$  undergoes addition of dimethylamide and methanethiolate to produce new complexes  $\text{Zn}^{\text{II}}(\text{OEBNMe}_2)$  and  $\text{Zn}^{\text{II}}(\text{OEBSMe})$  that contain a ring-opened tetrapyrrole as seen in Scheme 1. The products are sufficiently stable to be isolated and crystallized. In these complexes as well as in  $\text{Zn}^{\text{II}}(\text{OEBOMe})$ , the ligands adopt a helical geometry that is analogous to that seen in complexes of octaethylbiliverdin and octaethylformylbiliverdin. Some stereochemical aspects of the chiral nature of the helical ligand in complexes of the  $\text{Zn}^{\text{II}}(\text{OEBOR})$  family have been explored.<sup>32,33</sup> The formation of  $\text{Zn}^{\text{II}}(\text{OEBNMe}_2)$  provides a model for the initial stage of the reaction of ammonia with a 5-oxaporphyrin to yield 5-azaporphyrin. In this case the presence of the two alkyl groups on the amine prevents the further stages of the reaction that could lead to ring closure. Further information about the course of the conversion of a 5-oxaporphyrin to a 5-azaporphyrin might be obtained by examining the reaction of  $[\text{Zn}^{\text{II}}(\text{OEOP})](\text{O}_2\text{CCH}_3)$  with primary amines or the corresponding primary amides.

The crystallographic study makes it clear that  $\text{Zn}^{\text{II}}(\text{OEBSMe})$  possesses the open chain tetrapyrrole structure **4**. Thus, this complex has a structure analogous to those of  $\text{Zn}^{\text{II}}(\text{OEBOMe})$  and  $\text{Zn}^{\text{II}}(\text{OEBNMe}_2)$  rather than the macrocyclic structure **3**, as recently proposed.<sup>29</sup>

The electronic spectra shown in Figure 1 for the three complexes  $\text{Zn}^{\text{II}}(\text{OEBOMe})$ ,  $\text{Zn}^{\text{II}}(\text{OEBNMe}_2)$ , and  $\text{Zn}^{\text{II}}(\text{OEBSMe})$  display significant similarities, particularly the broad long-wavelength bands in the 800–900 nm region with an accompanying shoulder at shorter wavelength. These spectra can be taken as a simple tool for identifying compounds with the open chain structure **4**. By this criterion, the thiolate addition products reported in ref 29 also contain the open chain structure **4**.

## Experimental Section

**Preparation of Compounds.** The preparation of  $[\text{Zn}^{\text{II}}(\text{OEOP})](\text{O}_2\text{CCH}_3)$  followed the procedure outlined in an earlier paper.<sup>20</sup> Solvents were dried and degassed before use.

**$\text{Zn}^{\text{II}}(\text{OEBNMe}_2)$ .** Blue-green  $[\text{Zn}^{\text{II}}(\text{OEOP})](\text{O}_2\text{CCH}_3)$  (50.9 mg, 0.089 mmol) was dissolved in 50 mL of a mixture 1:1 (v/v), of tetrahydrofuran and dichloromethane under an atmosphere of dinitrogen. A 2.0 M solution of dimethylamine (0.8 mL, 0.39 mmol) in tetrahydrofuran was added to a separate flask under dinitrogen. A small piece of sodium was added to the dimethylamine solution, and after 10 min it was removed. The  $[\text{Zn}^{\text{II}}(\text{OEOP})](\text{O}_2\text{CCH}_3)$  solution was then transferred to the solution of sodium dimethylamide. The reaction solution was stirred for 48 h and formed a yellow-green solution. The reaction mixture was poured into 100 mL of dichloromethane and washed with water (3 × 100 mL). The dichloromethane solution was dried over sodium sulfate, filtered, and evaporated to dryness. The product was purified by flash chromatography on silica (25 mm × 150 mm) with 2% tetrahydrofuran in dichloromethane as eluant. The first band (yellow), which was near the solvent front, was discarded. The second band (also yellow), identified as  $\text{Zn}^{\text{II}}(\text{OEBNMe}_2)$ , was collected and evaporated to dryness; yield 4 mg, 8%. A third band, with an  $R_f$  value very near that of  $\text{Zn}^{\text{II}}(\text{OEBNMe}_2)$ , was identified as the

(32) Mizutani, T.; Yagi, S.; Honmaru, A.; Ogoshi, H. *J. Am. Chem. Soc.* **1996**, *118*, 5318.

(33) Mizutani, T.; Yagi, S.; Honmaru, A.; Murikami, S.; Ogoshi, H. *J. Org. Chem.* **1998**, *63*, 8769.

demetalated product H<sub>2</sub>OEBNMe<sub>2</sub>. For Zn<sup>II</sup>(OEBNMe<sub>2</sub>), UV/vis in dichloromethane: [ $\lambda_{\text{max}}$ , nm ( $\epsilon$ , M<sup>-1</sup> cm<sup>-1</sup>): 413, (30 800), 822, (12 000)]. <sup>1</sup>H NMR (300 MHz) (chloroform-*d*):  $\delta$  = 6.34 (s, 1H, meso proton), 6.10 (s, 1H, meso proton), 5.36 (s, 1H, meso proton), 3.12 (s, 6H, dimethylamido protons), 2.42 (m, 16 H, methylene protons), 1.1 (m, 12H, methyl protons), 1.04 (m, 12H, methyl protons). IR (KBr pellet; cm<sup>-1</sup>): 2960 s, 2930 s, 2860 s, 1730 w, 1700 w, 1650 s, 1600 s, 1570 s, 1530 m, 1520 m, 1450 m, 1390 m, 1380 m, 1300 w, 1270 s, 1200 s, 1150 m, 1120 m, 1050 w, 1000 s, 980 m, 950 m, 910 m, 820 w, 740 m. MALDI mass spectrum:  $m/z$  643.32 (M<sup>+</sup>).

**Zn<sup>II</sup>(OEBSMe).** Blue-green [Zn<sup>II</sup>(OEOP)](O<sub>2</sub>CH<sub>3</sub>) (26 mg, 0.039 mmol) and sodium methylthiolate (10 mg, 0.140 mmol) were placed in 20 mL of a 1:1 (v/v) solution of tetrahydrofuran and dichloromethane. After 1 h the solution changed color from blue to brown, which is indicative of the formation of Zn<sup>II</sup>(OEBSMe). The reaction solution was then filtered and poured into 100 mL of dichloromethane. The mixture was washed with water (3 × 100 mL). The dichloromethane solution was dried over sodium sulfate, filtered, and evaporated to dryness. The product was purified by flash chromatography on silica with 2% tetrahydrofuran in dichloromethane as eluant. The first band (yellow-green) was identified as H<sub>2</sub>OEBNMe<sub>2</sub>, the demetalated form of Zn<sup>II</sup>(OEBSMe). The second band (brown), containing the desired product Zn<sup>II</sup>(OEBSMe), was collected and evaporated to dryness; yield 12 mg, 54%. UV/vis in dichloromethane: [ $\lambda_{\text{max}}$ , nm ( $\epsilon$ , M<sup>-1</sup> cm<sup>-1</sup>): 441, (22 100), 846, (7850)]. <sup>1</sup>H NMR (300 MHz) (dichloromethane-*d*<sub>2</sub>):  $\delta$  = 6.46 (s, 1H, meso proton), 6.35 (s, 1H, meso proton), 5.38 (s, 1H, meso proton), 2.86 (s, 3H, methanethiolate protons), 2.43 (m, 12H, methylene protons), 2.15 (m, 4H, methylene protons), 1.13 (m, 12H, methyl protons), 0.97 (m, 12H, methyl protons). IR (KBr pellet; cm<sup>-1</sup>): 2960 s, 2930 m, 2870 w, 1710 w, 1660 m, 1570 s, 1530 m, 1460 w, 1450 w, 1380 s, 1300 w, 127 m, 1210 s, 1150 w, 1110 m, 1050 w, 1010 s, 950 m, 910 m. MALDI mass spectrum:  $m/z$  645.9 (M<sup>+</sup>).

**X-ray Data Collection for Zn<sup>II</sup>(OEBNMe<sub>2</sub>).** Crystals were obtained by layering a tetrahydrofuran solution of Zn<sup>II</sup>(OEBNMe<sub>2</sub>) over a layer of water in a 5 mm glass tube. Slow diffusion of water into the tetrahydrofuran solution of the complex produced dark green plates. A plate was coated with a light hydrocarbon oil and mounted in the 130 K dinitrogen stream of a Siemens P4 diffractometer equipped with a LT-2 low-temperature apparatus. Intensity data were collected using nickel-filtered Cu K $\alpha$  radiation. Crystal data are given in Table 2. Two check reflections showed only random (<1%) variation in intensity during data collection. The data were corrected for Lorentz and polarization effects. Further details are given in the Supporting Information.

**X-ray Data Collection for Zn<sup>II</sup>(OEBSMe).** Crystals were obtained by layering a tetrahydrofuran solution of Zn<sup>II</sup>(OEBSMe) over a layer of water in a 5 mm glass tube. Slow diffusion of water into the tetrahydrofuran solution of the complex produced dark brown needles. Data collection was carried out on a Syntex P2<sub>1</sub> diffractometer that was equipped with a locally modified LT-1 low-temperature apparatus. Graphite-monochromated Cu K $\alpha$  radiation was employed. Other methods followed those described above.

**Table 2.** Crystal Data and Data Collection Parameters for Zn<sup>II</sup>(OEBNMe<sub>2</sub>) and Zn<sup>II</sup>(OEBSMe)

	Zn <sup>II</sup> (OEBNMe <sub>2</sub> )	Zn <sup>II</sup> (OEBSMe)
empirical formula	C <sub>37</sub> H <sub>49</sub> N <sub>5</sub> OZn	C <sub>36</sub> H <sub>46</sub> N <sub>4</sub> OSZn
fw	645.18	648.20
color and habit	black plate	dark green needle
cryst syst	triclinic	monoclinic
space group	<i>P</i> 1̄	<i>P</i> 2 <sub>1</sub> / <i>n</i>
<i>a</i> , Å	9.8828 (8)	14.134 (3)
<i>b</i> , Å	13.846 (2)	16.819 (4)
<i>c</i> , Å	14.054 (3)	14.848 (3)
$\alpha$ , deg	112.692 (10)	90
$\beta$ , deg	95.451 (9)	107.85 (2)
$\gamma$ , deg	105.076 (10)	90
<i>V</i> , Å <sup>3</sup>	1671.4 (4)	3359.8 (13)
<i>T</i> , K	130(2)	130(2)
<i>Z</i>	2	4
<i>d</i> <sub>calcd</sub> , g cm <sup>-3</sup>	1.282	1.281
radiation, Å	CuK $\alpha$ , (1.54178 Å),	CuK $\alpha$ , (1.54178 Å),
$\mu$ , mm <sup>-1</sup>	1.294	1.848
range of transm factors	0.78–0.97	0.49–0.91
no of unique data	4422	5573
no. of params refined	407	397
R1 <sup>a</sup>	0.076	0.101
wR2 <sup>b</sup>	0.23	0.287

<sup>a</sup> R1 =  $\sum ||F_o| - |F_c|| / \sum |F_o|$ , (obsd data,  $I > 2\sigma(I)$ ). <sup>b</sup> wR2 =  $[\sum [w(F_o^2 - F_c^2)^2] / \sum [w(F_o^2)^2]]^{1/2}$  (all data).

**Solution and Structure Refinement.** Calculations were performed with the SHELXTL 5 series of programs. Scattering factors and correction for anomalous dispersion were taken from a standard source.<sup>34</sup> An absorption correction was applied to each structure.<sup>35</sup> The solutions were determined by direct methods and subsequent cycles of least-squares refinement and calculation of difference Fourier maps.

**Instrumentation.** <sup>1</sup>H NMR spectra were recorded on a General Electric QE-300 FT NMR spectrometer operating in the quadrature mode (the <sup>1</sup>H frequency is 300 MHz). Electronic spectra were obtained using a Hewlett-Packard diode array spectrometer.

**Acknowledgment.** We thank the NIH (Grant GM-26226) for financial support and Professor L. Latos-Graożyński, Dr. S. Attar, and Dr. R. Koerner for helpful discussions.

**Supporting Information Available:** Tables giving X-ray crystallographic data for Zn<sup>II</sup>(OEBNMe<sub>2</sub>) and Zn<sup>II</sup>(OEBSMe). This material is available free of charge via the Internet at <http://pubs.acs.org>.

IC9904283

(34) *International Tables for Crystallography*; Wilson, A. J. C., Ed.; Kluwer Academic Publishers: Dordrecht, The Netherlands, 1992; Vol. C.

(35) Parkin, S.; Moezzi, B.; Hope, H. J. *Appl. Crystallogr.* **1995**, 28, 53.